Phase Transitions in *N*-Propylpyridinium-TCNQ Ion-radical Complex Salts

Mutsuaki MURAKAMI* and Susumu YOSHIMURA
Matsushita Research Institute Tokyo, Inc., Ikuta, Tama-ku, Kawasaki 214
(Received March 27, 1980)

N-Propylpyridinium $(TCNQ)_x$ crystallized in two complex salts ($x=2$, 2.5), both of which displayed initial irreversible and subsequent reversible first-order phase transitions with a sharp discontinuity in the electrical conductivity. The reversible transitions of both salts are essentially the same in spite of their differences in stoichiometry. The transitions were accompanied by crystal structure changes; the changes in the physical properties were ascribed to the crystalline distortion in both the one-dimensional TCNQ chain and the motion of the cation molecules. The high-temperature phase was metallic, with a zero activation energy for conduction; the source of the metallic behavior was also discussed. The electronic and infrared absorption spectra suggest that the high-temperature modification has a less distorted stacking of TCNQ molecules in the column.

The phase transitions and metallic conductivity in a quasi-one-dimensional system based on 7.7.8.8-tetracyanoquinodimethane (TCNQ) ion-radical salts have been the subject of extensive investigation. The highly conducting salts of TCNQ with *N*-methylphenazinium (NMP(TCNQ)),[1,2] quinolinium $(Q(TCNQ)_2)$[3,4] and acridinium $(Ad(TCNQ)_2)$[5] display a metal-insulator (M-I) transition characterized by a smooth maximum in the conductivity. The metallic behavior of these salts has been explained in various manners: a mobility model in which the conductivity is defined as the product of the concentration of charge carriers and the mobility of the carriers,[6] diffusion through the localized state by means of a disorder effect,[7-9] inter-strand hopping due to the finite length of the conducting chains,[10,11] and an M-I transition with a single particle gap going to zero.[1]

On the other hand, there are some examples of first-order phase transitions which display a discrete change in the electrical conductivity. Reversible transitions are found in alkali-metal (TCNQ),[12,13] methyltriphenylphosphonium $(TCNQ)_2$,[14] and *N*-ethyl·*N*·methylmorpholinium $(TCNQ)_2$,[15,16] $(MEM(TCNQ)_2)$, while monotropic transitions are found in *N*-methylquinolinium $(TCNQ)_x$[17] and methyldiethylcyclohexylammonium $(TCNQ)_2$.[18] They have been understood on the basis of crystallographic change, Adler-Brooks transition,[19,20] spin Peierls transition, or transition from a metastable to a stable form.[21]

In a previous paper, we reported that substituted pyridinium and picolinium–TCNQ complex salts exhibited a variety of first-order phase transitions.[22] The irreversible transition was correlated to the appearance of multiple forms, while the reversible one manifested itself for specific cations. *N*-propylpyridinium $(TCNQ)_x$, $(NPPy(TCNQ)_x)$ complex salts crystallized in two forms ($x=2.5$ and 2.0) displayed two kinds of first-order phase transitions, *viz.*, an initial irreversible transition, and subsequent reversible transitions. In this paper, we will report on the electrical, optical, and magnetic properties of the transitions, and will discuss the transition mechanism and the source of the metallic behavior in the high-temperature phase.

Experimental

Preparation of NPPy(TCNQ)$_x$ Complex Salts. NPPy-$(TCNQ)_x$ complex Salt II was synthesized from *N*-propylpyridinium iodide and three-halves molar excess of TCNQ using one of the methods generally described by Melby *et al.*[23] After the salt had been synthesized, recrystallization was done in highly purified acetone at 0 °C. The formation of the two salts was controlled by the crystallization conditions: the Salt I was obtained from a concentrated solution (50 mmol dm^{-3}) with rapid crystallization as a fine needle form, while the Salt II was recrystallized by slow crystallization from a dilute solution (30 mmol dm^{-3}) as a rod or triclinic prism form.

The cation-to-TCNQ ratio of the complex salts was estimated by the spectral analysis from a simple salt of NPPy-(TCNQ) and neutral TCNQ.[21] The value of the molar excitation coefficient for TCNQ in highly purified acetonitrile was 67000 mol^{-1} dm^3 cm^{-1} at the wavelength of 395 nm, while the coefficients of $TCNQ^-$ were 26300 and 46100 mol^{-1} dm^3 cm^{-1} at 420 and 842 nm respectively; the coefficient at 395 nm was 21200 mol^{-1} dm^3 cm^{-1}. From the analysis, the cation-to-TCNQ ratio of I is estimated to be 2.48, and that of II, to be 1.94. The elemental analysis values for I were; Found: C, 72.32; H, 3.43; N, 24.43%, calcd for $(C_8H_{12}N)_2(C_{12}H_4N_4)_5$: C, 72.15; H, 3.48; N, 24.36%, while those for II were; Found: C, 72.62; H, 3.70; N, 23.48%, calcd for $(C_8H_2N)(C_{12}H_4N_4)_2$: C, 72.45; H, 3.77; N, 23.77%. From these results, considering the experimental error, we decided the cation-to-TCNQ ration to be 2.5 for I and 2.0 for II.

Electrical Measurements. The specific resistivities of compactions were determined with a resistivity measuring apparatus, Kokusai Electric Co., Ltd., Model VR4. The temperature dependence of the electrical resistivity along three crystallographic directions of a single crystal was measured with an ordinary four-point method with gold wires (0.05 mmϕ) and silver paste (duPont conductive silver coating material No. 4929). The sample was mounted in an evacuated glass cell sealed with a hermetic seal (NEC No. S110). The temperature was regulated with thermostat equipment (Sigma Electric Co., Ltd., Model TE-307S) and a temperature sweeper (Model SP-9D) at the sweep rate of 0.1—2.0 °C/min in the temperature range of 210—430K.

Other Measurements. The infrared absorption spectra were measured at various temperature with a Hitachi grating infrared spectrometer Model No. 215, in the wave number range between 4000 and 650 cm^{-1}. The solid state electronic absorption spectra were measured in the range between 5000 and 44000 cm^{-1} with a Cary spectrometer, Model No. 14. Samples were fully ground and carefully rubbed on a substrate; a quartz plate for measurements in the electronic region or a sodium chloride plate, for those in the infrared region.

Measurements of differential scanning calorimetry (DSC) were made with a Shimadzu thermoflex apparatus, SC-20, in a nitrogen atomosphere at the sweeping rate of 0.5—2.0 °C/

min in the temperature range of 293—430K. The data employed were an average value of ten measurements.

The powder X-ray diffraction patterns were measured with a Philips PW-1051 X-ray diffractometer by the use of the Cu·$K\alpha$ line.

The magnetic susceptibility was measured on a magnetic balance using Faraday's method in the temperature range of 100—430K. The sample, a pressed pellet about 100 mg, was placed in a quartz cell, and measurement was made under a vaccum. The absolute value of the susceptibility was estimated from gadrinium oxide ($\chi=135\times10^{-6}$ emu/g) placed in the same quartz cell. The paramagnetic contribution (χ_{para}) to the susceptibility was determined from the difference of $\chi-\chi_{dia}$, while the diamagnetic contribution, χ_{dia}, was estimated from Pascal's rule.

Results and Discussion

Electrical Properties of NPPy(TCNQ)$_x$ Salts. The most typical difference between the two salts, besides stoichiometry and morphology, is the resistivity at room temperature; the specific resistivity of the powder smaple I ($x=2.5$) was 1.4 Ω cm, while that of the II ($x=2.0$) was 2000 Ω cm. In the Salt II, the lowest resistivity is found in the direction of the a-axis (1000 Ω cm), and the resistivity anisotropy ratio of the a, b, and c axes was 1 : 24 : 4.5. On the other hand, the lowest resistivity of I was found in the long axis (0.12 Ω cm) and its anisotropy ratio is expected to be larger than that of II.

The Temperature Dependence of the Resistivity of II. The temperature dependence of the electrical resistivity along each crystallographic direction of II was measured; the results are shown in Fig. 1. The resistivity abruptly changed at three temperatures; the resistivity jump observed at 383 K by initial heating was irreversible, while the other two jumps, at 370 K and 376 K, were the portions of a hysteresis loop of a reversible transition. We recognized two kinds of phase transitions and three distinct phases; it will be convenient to identify the phases as α_{II}, β', β as is indicated in the figure.

For example, in the c-direction, the inclination of the $\log\rho$-T^{-1} curve in the semiconducting α_{II} phase increased with the temperature, from 0.18 eV in the temperature range of 200—230 K to 0.42 eV in the range of 330—370 K. On the other hand, the β' phase was metallic in the sense that it had a zero temperature coefficient of resistivity. The β phase was semiconducting, with an activation energy of 0.54 eV between 320 and 350 K, which was larger than that of the α_{II} phase in the same temperature range. A decrease in the activation energy was also observed at lower temperatures; the value was 0.16 eV in the temperature range of 200—230 K.

The features of the ρ-T characteristic for the three crystallographic directions closely resembled each other. Some quantitative differences between these crystal axes are summarized as follows: 1) The magnitudes of the resistivity jumps at the irreversible transitions were factors of 23, 140, and 45 for the a, b, and c axes respectively. 2) In the high-temperature β' phase, the resistivities were 2, 8, and 4 Ω cm for the a, b, and c axes respectively. The maximal anisotropy ratio in this phase was only 4, which is to be compared with that of the α_{II} phase, 24. 3) The a- and c-axis conductivity in the β' phase had a zero activation energy, while the b-axis one had a small positive value of 0.09 eV. 4) The magnitudes of the resistivity jumps in the reversible transition at 376 K were factors of about 12, 20, and 8 for the a, b, and c axes respectively. The maximal anisotropy ratio in the β phase at 293 K was reduced to about 20.

Crystal Structure Change of II. The very sharp resistivity change shown in Fig. 1 suggests a first-order phase transition, and, in fact, latent heat was observed at three temperatures with the DSC experiment. The results for ΔH were +13.81, −9.83, and +10.13 kJ mol^{-1} for the $\alpha_{II}\rightarrow\beta'$, $\beta'\rightarrow\beta$, and $\beta\rightarrow\beta'$ transitions respectively, and the corresponding entropy changes (ΔS) were +35.98, −26.57, and +26.69 J K^{-1} mol^{-1}.

Powder X-ray experiments were made at three temperatures corresponding to the three phases: the α_{II}

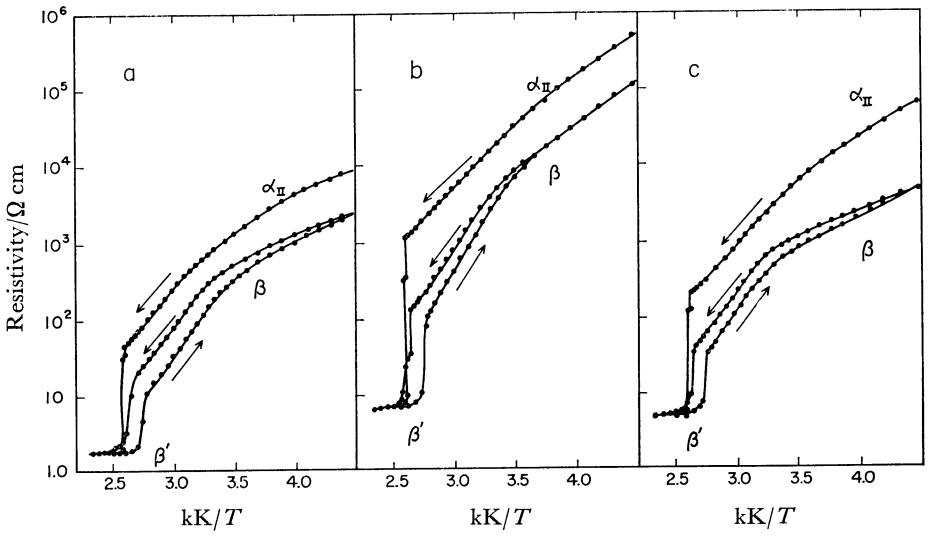

Fig. 1. Temperature dependence of the electrical resistivity of Salt-II along the a, b, c-directions.

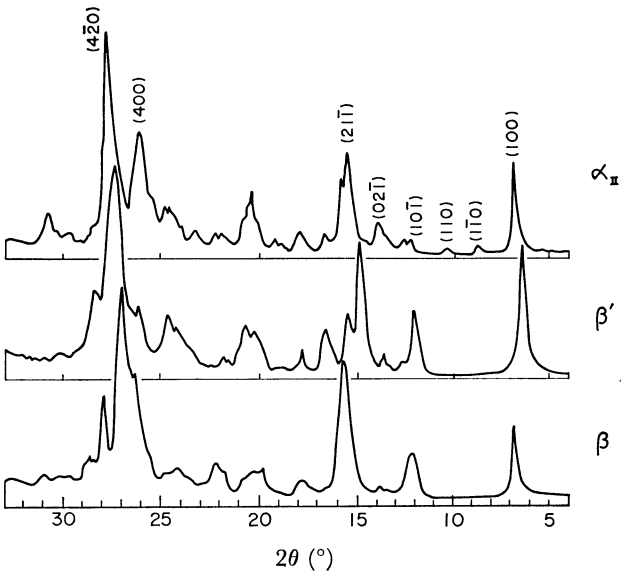

Fig. 2. Powder X-ray diagrams of α_{II} (293 K), β' (393 K), and β (293 K) modifications of Salt-II.

phase, 293 K, the β' phase, 399 K, and the β phase, 293 K. The results are shown in Fig. 2. The three X-ray diagrams of the α_{II}, β', and β phases were entirely different form each other, which confirms that the transitions are crystallographic phase transitions. Though a detail discussion of the crystal structure change must await a full crystal structure analysis of the β' and β phases, we can provide a rough view of the structure change as inferred from the shifts of the characteristic lines on the powder X-ray patterns. The most remarkable change at the $\alpha_{II} \rightarrow \beta'$ transition is observed in the lower angle region than 10°. From the crystal structure analysis of the α_{II} phase,[24] the relation between the lines and the reflection plane was calculated. The α_{II} belongs to the triclinic system with the space group P1 or P$\bar{1}$ and the lattice constants $a=14.542$, $b=13.723$, $c=7.802$ Å, $\alpha=104.06°$, $\beta=110.72°$, $\gamma=94.08°$ and $z=2$. The intense line at the lowest angle, 6.60°, is a (100) reflection, while the lines at 8.6° and 10.2° are reflections from (1$\bar{1}$0) and (110) respectively. In the β' phase, the lines corresponding to (1$\bar{1}$0) and (110) reflections disappeared, and only an intense line at 6.08° was observed in this region. The results indicate the change in the crystal symmetry: from a triclinic crystal (α_{II} phase) to a monoclinic crystal (β' phase). On the contrary, the crystal symmetry did not change at the $\beta' \leftrightarrows \beta$ transition, because the β phase had only a new line appearing at 6.55°. If these lines correspond to the (100) reflection, it means that the β' phase has the largest (100) spacing. The average inter-TCNQ column distance increased during the $\alpha_{II} \rightarrow \beta'$ transition and decreased during the $\beta' \rightarrow \beta$ transition. The large change in the interchain distance suggests that the rotation of cation molecules plays an important role at these transitions.

The most intense line in the α_{II} phase at 27.7° or the distance of about 3.2 Å originates from a spacing or paired TCNQ[24] in the TCNQ column. If the most intense reflection in the β' phase at 27.2° also comes from a plane nearly parallel to the TCNQ planes, the shift of this line with the $\alpha_{II} \rightarrow \beta'$ transition corresponds to a 1.8% increase in the inter-planar spacing of paired TCNQ molecules. Therefore the resistivity change at the $\alpha_{II} \rightarrow \beta'$ transition can be explained by the change in the stacking mode of TCNQ molecules from diadic to monadic configurations. In the β phase, the reflection appears at 27.0°; it undergoes an increase of about 0.7% in the spacing at the $\beta' \rightarrow \beta$ transition. The change in the interplanar spacing of TCNQ molecules at the reversible transition well explains the resistivity change.

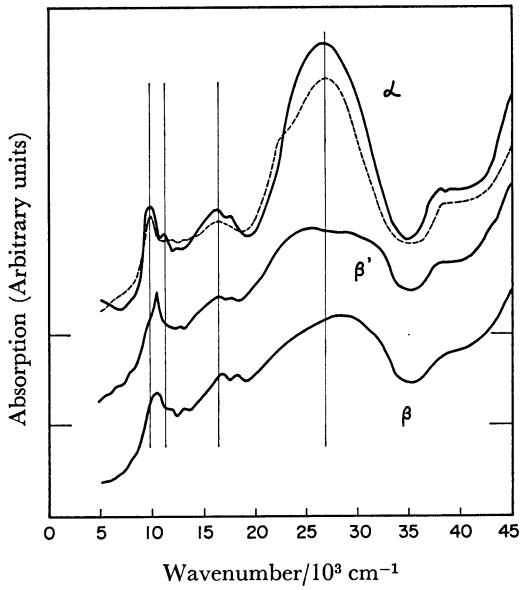

Fig. 3. Electronic absorption spectra of α (293 K), β' (393 K), and β (293 K) modifications of Salt-II (——) and Salt-I (------).

Change in TCNQ Column Structure of II. Figure 3 shows the electronic absorption spectra of a powder film rubbed over a quartz plate at three temperatures corresponding to the α_{II}, β', and β phases. The spectrum of the α_{II} phase was characterized by a strong intramolecular absorption centered at 26800 cm^{-1} (local excitation band, LE_2)[25] and a relatively strong absorption at about 16000 cm^{-1}. The latter may be interpreted as an intramolecular transition of a TCNQ molecule (LE_1) and/or an absorption of associated TCNQ molecules.[26] In general, the absorption band at around 10000 cm^{-1} has been interpreted in various manners: as an intermolecular charge transfer transition of $TCNQ^-$ to $TCNQ^-$,[27] as a transition to an upper band distinguished from a near infrared absorption which is due to an intraband transition, or as an interaction between LE_1 and CT_1. The doubly splitting band at 10000 cm^{-1} and 11300 cm^{-1} may be due to an interaction of LE_1 and CT_1 by analogy of the electronic spectra of $TEA(TCNQ)_2$; the band splitting suggests the crystallographic inequivalence of the TCNQ molecules in the column.

The absorption spectrum of the β' phase differed from those of the α phase, in which it had a weaker absorption in the intramolecular excitation regions at around 25000

cm^{-1} and in which the absorption located at around 10000 cm^{-1} had a single sharp peak at 10400 cm^{-1}. The remarkable change in the intramolecular absorption may explain the increase in the conductivity in the β' phase. The change of the spectrum around 10000 cm^{-1} shows the change of the TCNQ column, namely, the structure at the β' phase is almost equivalent which implies that the negative charge may delocalize throughout the TCNQ column. In the case of such a column structure, the CT_1 absorption band does not appear; in fact, $Q(TCNQ)_2$ and NMP(TCNQ) show only a single LE_1 peak at around 10000 cm^{-1}. The spectrum of the β phase was characterized by an intramolecular absorption band at 28000 cm^{-1} and splitting bands at 10100 cm^{-1} and 11400 cm^{-1} (shoulder). The latter bands indicate the presence of crystallographic inequivalency in the TCNQ column.

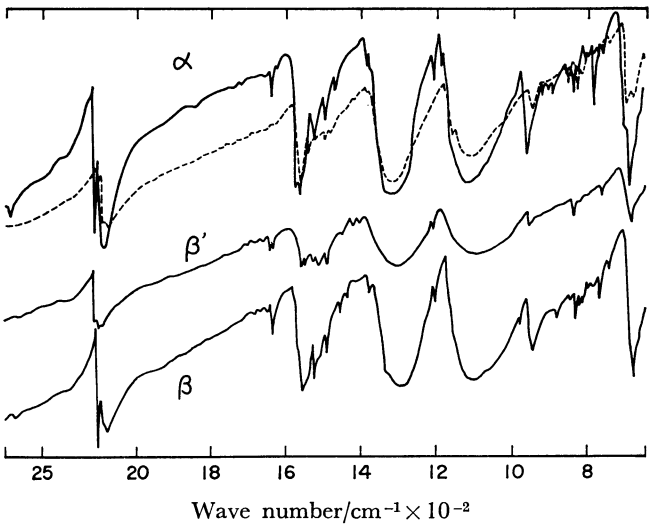

Fig. 4. Infrared absorption spectra of α (293 K), β' (393 K), and β (293 K) modifications of Salt-II (——) and Salt-I (------).

Similar results for the arrangement of TCNQ molecules were obtained from the infrared measurement.[28,29] The results are shown in Fig. 4. The α_{II} and β phases had sharp molecular absorption bands of TCNQ in the C≡N stretching regions around 2200 cm^{-1}, which indicates the presence of localized TCNQ molecules in the column. In the β' phase, sharp C≡N stretching absorptions were absent and the C–H bending band centered at 1290 cm^{-1} and the C–CN stretching band (1100 cm^{-1}) were broader and located at lower energies as compared with the α_{II} and β phases. The shift of the bands shows the decreased intermolecular repulsion or contraction of the electronic band gap, while the broadening of the bands may be due to the increased electronic band, which broadened to the infrared region. Thus, we concluded that the α_{II} and β phases have a disordered arrangement of TCNQ molecules, whereas the β' phase has an almost ordered stack of TCNQ molecules.

Metallic Nature of II in the β' Phase. The results of the ρ-T characteristics for the reversible $\beta \rightleftarrows \beta'$ transition are similar to those found in VO_2, which has offered a good example of a crystalline distortion or Adler-Brooks model.[30,31] The optical data which have suggested a pairing of TCNQ molecules at low temperatures are consistent with the increased resistivity of the β phase, because such a pairing opens an energy gap, as in the case of VO_2. The rough coincidence in both the transition temperature, T_0, and the activation energy for conduction just below, T_0, is noteworthy: II, 376 K and 0.51 eV, and VO_2 339 K and 0.50 eV.[32] However, a more exact examination may lead to the conclusion that the phase transition of our salt cannot be described by this mode. The Adler-Brooks model predicts that the energy gap, E_{g0}, due to a crystalline distortion is proportional to T_0, provided that the band widths are not very different. If we take $E_{g0}/kT_0=10$ as a rough estimate, the measured T_0 (376 K) gives an energy gap of 0.32 eV. Note that the observed activation energy, 0.51 eV (c-axis), is considerably larger than the predicted one, 0.16 eV. This discrepancy indicates the inapplicability of the Adler-Brooks model.

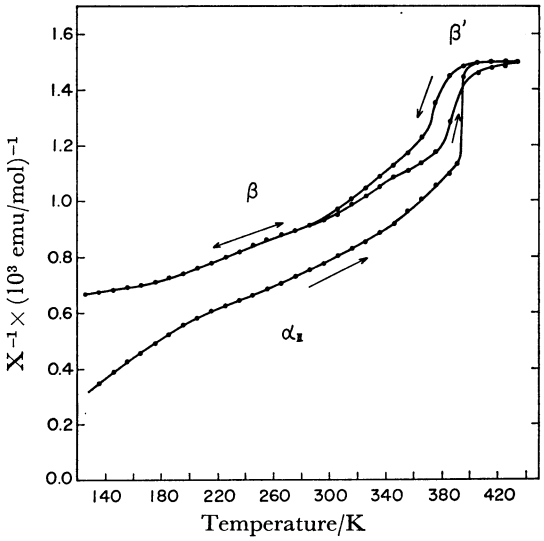

Fig. 5. Temperature dependence of the inverse paramagnetic susceptibility of Salt-II.

Figure 5 shows the temperature dependence of the paramagnetic susceptibility for the temperature range of 100—430 K. The results show discrete changes in χ which correspond to the resistivity jumps found in Fig. 1. The β' phase had a temperature independent susceptibility of about 5.0×10^{-4} emu/mol. The low-temperature α_{II} and β phases, on the other hand, exhibited Curie-Weiss like behavior, with a marked increase in the paramagnetic susceptibility at low temperatures.

The observed magnetic behavior cannot be described by ferromagnetic impurities, for the low-temperature α_{II} and β phases did not have the same magnitude of susceptibility. Indeed, the effective Curie-Weiss behavior may be explained by an array of disordered paramagnetic moments. The reason for this speculation is that the hopping motion of a localized electron is suggested by the fact that the activation energy around

370—300 K is considerably larger than that predicted by the Adler-Brooks model. Other reasons are that the NPPy cation is assymmetric and II was crystallized as a metastable crystal. The decrease in the magnitude of χ with the $\alpha_{II} \rightarrow \beta$ transition indicated that the crystal structure was made less ordered with the irreversible transition, which is consistent with the crystallographic and optical data.

The observed behavior of the paramagnetic susceptibility of the β' phase is likely to be connected with the Pauli spin susceptibility of the free electron system, and this seems to provide evidence that the β' phase is indeed metallic. However, the weak temperature dependence of the paramagnetic susceptibility of highly conducting TCNQ salts can also be described by the properties of a one-dimensional Mott insulator[33] or by those of a tight binding band.[34] In these cases, the electronic states have been thought to be localized at a lattice point in the one-dimensional TCNQ chain. Moreover, the disorder model can explain the observed behavior with an expression in the form of $\chi = \chi_{para} + \chi_{curie-weiss}$. Several data presented above suggest that the β' phase may also be described by a localized electronic model. For example, the intramolecular absorption band at 16000 cm^{-1} (Fig. 3) has a doublet peak, which indicates that the β' phase does not have a completely uniform stacking of the TCNQ molecule. This may be understood on the basis of the highly asymmetric structure of the cation molecule, which makes a major contrast to the case of MEM-$(TCNQ)_2$.[15,16] At this stage, we surmise that the β' phase is described by the phonon-assisted hopping between localized states. The relatively high and temperature-independent conductivity agrees well with the expected values of the minimum resistivity by hopping (order of 1 Ω cm) and the small temperature slope of the resistivity ($(\partial\rho/\partial T = 1.2 \times 10^{-3}$ Ω cm K^{-1}).[5]

Phase Transitions of I. The temperature dependence of the electrical resistivity of a powder sample of I ($x=2.5$) is shown in Fig. 6. An irreversible transition appeared in a broad temperature range starting at about 390 K, where the resistivity increased by a factor of about 5. Since the transition temperature was varied by the rate of the rise in the temperature or by the crystal perfection, the transition is a polymorphic transition from an unstable to a stable form. After the irreversible transition was completed, the salt displayed a reversible transition similar to that of II. We can also recognize three phases, so we indicates the phases as α_I, β', and β, as is indicated in the figure.

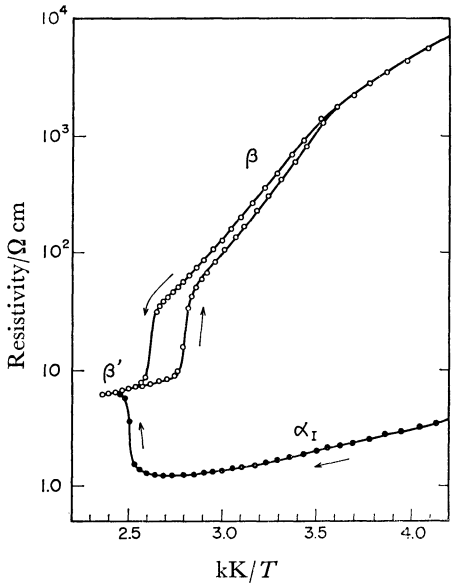

Fig. 6. Temperature dependence of the electrical resistivity of Salt-I (pressed rod), irreversible change (-●-●-), reversible change (-○-○-).

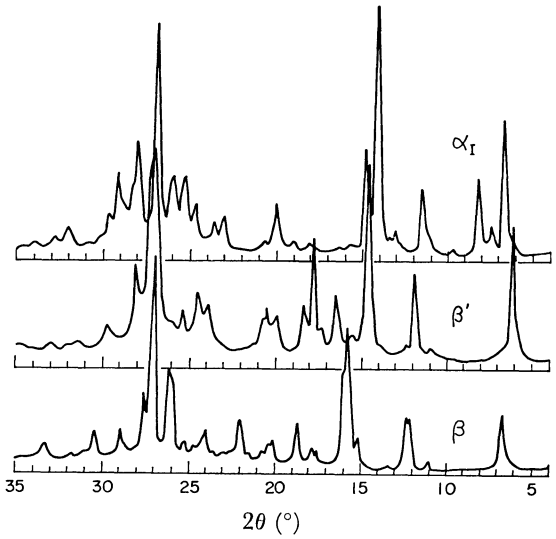

Fig. 7. Powder X-ray diagrams of α_I (293 K), β' (393 K), and β (293 K) modifications of Salt-I.

The powder X-ray diffraction patterns of I are shown in Fig. 7. The pattern of the α_I phase is quite different from that of the α_{II} phase, but the patterns of the β' or β phase of I and II are identical. During the $\alpha_I \rightarrow \beta'$ transition, a distinct change was observed at the most intense line around 26.8°, which implies that the average distance between TCNQ molecules expanded at the $\alpha_I \rightarrow \beta'$ transition. The electronic and infrared absorption spectra of I are shown by dotted lines in Figs. 3 and 4 respectively. The infrared spectrum of the α_I phase was characterized by broader bands located at a lower energy region as compared with the characteristic bands of TCNQ of the α_{II} phase. The electronic spectrum of the α_I phase was characterized by an absorption located at around 10000 cm^{-1}, in which the band splitting was not clear and the second peak was shouldered. The results indicate that the TCNQ column at the α_I phase is less distorted than that of the α_{II} phase and that TCNQ molecules are stacked almost uniformly. The conductivity change of the $\alpha_I \rightarrow \beta'$ transition is well explained by these results.

A difference in the ρ-T characteristic of I from that of II was the activation energy for conduction in the β' phase: 0 eV for II and 0.10 eV for I. Although I has quite a different stoichiometry from that of II, the same crystal structure may be realized by discarding one cation out of the five cation molecules from the structure of II.

If the crystal structure of I is characterized by such large defects in the cation column, the difference in the activation energies in the β' phase may be explained by such defects.

The authors offer their thanks to Dr. Ichimin Shirotani of Tokyo University and to Prof. Hayao Kobayashi of Tōhō University for their stimulating discussions. They are also indebted to Dr. Michiko Konno of Tokyo University for providing them with the details of the crystal structure of NPPy(TCNQ)$_x$, II.

References

1) L. B. Coleman, J. A. Cohen, A. F. Garito, and A. J. Heeger, *Phys. Rev. B*, **7**, 2122 (1973).
2) A. J. Epstein, E. M. Conwell, D. J. Sandman, and J. S. Miller, *Solid State Commun.*, **23**, 355 (1977).
3) L. I. Buravov, D. N. Fedutin, and I. F. Schegolev, *Sov. Phys. JETP.*, **32**, 612 (1971).
4) K. Holczer, G. Mihaly, A. Janossy, and G. Grüner, *Mol. Cryst. Liq. Cryst.*, **32**, 199 (1976).
5) G. Mihaly, K. Ritvay-Emandity, and G. Grüner, *J. Phys. Chem.*, **8**, L361 (1975).
6) A. J. Epstein, E. M. Conwell, and J. S. Miller, *Ann. N. Y. Acad. Sci.*, **313**, 183 (1978).
7) A. N. Bloch, R. B. Weisman, and C. M. Varma, *Phys. Rev. Lett.*, **28**, 753 (1972).
8) E. Ehrenfreund, S. Etemad, L. B. Coleman, E. F. Rybaczewski, A. F. Garito, and A. J. Heeger, *Phys. Rev. Lett.*, **29**, 269 (1972).
9) Gogolin, A. A., S. P. Zolotuhin, V. I. Melnikov, E. I. Rashba, and I. F. Shchgolev, *JETP Lett.*, **22**, 278 (1975).
10) E. Ehrenfreund, E. F. Rybaczewski, A. F. Garito, and A. J. Heeger, *Phys. Rev. Lett.*, **28**, 873 (1972).
11) M. J. Rice and J. Bernasconi, *J. Phys. F*, **3**, 55 (1973).
12) J. G. Vegter and J. Kommandeur, *Mol. Cryst. Liq. Cryst.*, **30**, 11 (1975).
13) M. Konno, T. Ishii, and Y. Saito, *Acta Crystallogr., Sect. B*, **33**, 763 (1977).
14) Y. Iida, *J. Chem. Phys.*, **59**, 1607 (1973).
15) S. Huizinga, J. Kommandeur, G. A. Sawatzky, B. T. Thole, K. Kopinga, W. J. M. de Jonge, and J. Roos, *Phys. Rev. B*, **19**, 4723 (1979).
16) A. Bosh and B. Van Bodegom, *Acta Crystallogr., Sect. B*, **33**, 3013 (1977).
17) M. Murakami and S. Yoshimura, *J. Phys. Soc. Jpn.*, **38**, 488 (1975).
18) J. C. Giuntini, D. Jullien, and J. V. Zanchetta, *Mol. Cryst. Liq. Cryst.*, **32**, 203 (1976).
19) D. Adler and H. Brooks, *Phys. Rev.*, **155**, 826 (1967).
20) J. G. Vegter and J. Kommandeur, *The AIP Conf. Proc.*, **No. 10**, 1525 (1972).
21) M. Murakami and S. Yoshimura, *Bull. Chem. Soc. Jpn.*, **48**, 157 (1975).
22) M. Murakami and S. Yoshimura, *Chem. Lett.*, **1977**, 929.
23) L. R. Melby, R. J. Harder, W. R. Hertler, W. Mahler, R. E. Benson, and W. E. Mochel, *J. Am. Chem. Soc.*, **84**, 3374 (1962).
24) M. Konno and Y. Saito, *Proc. Symp. Molecular Structure*, Tokyo, Oct. 9—12 (1979), p. 20.
25) J. Tanaka, M. Tanaka, T. Kawai, T. Takabe, and O. Maki, *Bull. Chem. Soc. Jpn.*, **49**, 2358 (1976).
26) J. G. Vegter and J. Kommandeur, *Phys. Rev. B*, **9**, 5150 (1974).
27) J. B. Torrance, B. A. Scott, and F. B. Kaufman, *Solid State Commun.*, **17**, 1369 (1975).
28) K. Kondow and T. Sakata, *Phys. Status Solidi A*, **6**, 551 (1971).
29) B. Lunelli and C. Pecile, *J. Chem. Phys.*, **52**, 2375 (1970).
30) D. Adler, "Solid State Physics," ed by F. Seitz, D. Turnbell, and H. Ehrenreich, Acad. Press, New York (1968), Vol. 21.
31) A. Zylbersztejn and N. F. Mott, *Phys. Rev. B*, **11**, 4383 (1975).
32) D. Adler, J. Feinleib, H. Brooks, and W. Paul, *Phys. Rev.*, **155**, 851 (1967).
33) L. N. Bulaeuskii, A. V. Zvarykina, Yu. S. Karimov, R. B. Lyubouskii, and I. F. Schegolev, *Zh, Eksp. Teor. Fiz.*, **62**, 725 (1972); [*Soviet Phys. JETP*, **35**, 384 (1972)].
34) A. H. Kahn, G. A. Candela, V. Waltka, Jr, and J. H. Perlstein, *J. Chem. Phys.*, **60**, 2264 (1974).